2018

The effect of DNA backbone on the triplet mechanism of UV-induced thymine-thymine (6-4) dimer formation

Xingyong Wang
University of Wollongong, xingyong@uow.edu.au

Haibo Yu
University of Wollongong, hyu@uow.edu.au

Publication Details

Wang, X. & Yu, H. (2018). The effect of DNA backbone on the triplet mechanism of UV-induced thymine-thymine (6-4) dimer formation. Journal of Molecular Modeling, 24 (11), 319-1-319-9.

The effect of DNA backbone on the triplet mechanism of UV-induced thymine-thymine (6-4) dimer formation

Abstract
Density functional theory calculations have been carried out to investigate the formation mechanism of the thymine-thymine (6-4) dimer ((6-4)TT), which is one of the main DNA lesions induced by ultraviolet radiation and is closely related to skin cancers. The DNA backbone was found to have nonnegligible effects on the triplet reaction pathway, particularly the reaction steps involving substantial base rotations. The mechanism for the isomerisation from (6-4)TT to its Dewar valence isomer (DewarTT) was also explored, confirming the necessity of absorbing a second photon. In addition, the solvation effects were examined and showed considerable influence on the potential energy surface.

Disciplines
Medicine and Health Sciences

Publication Details
Wang, X. & Yu, H. (2018). The effect of DNA backbone on the triplet mechanism of UV-induced thymine-thymine (6-4) dimer formation. Journal of Molecular Modeling, 24 (11), 319-1-319-9.

The effect of DNA backbone on the triplet mechanism of UV-induced thymine-thymine (6–4) dimer formation

Xingyong Wang[1,2]*, Haibo Yu[1,2,3]*

*Email: xingyong@uow.edu.au, hyu@uow.edu.au

[1] School of Chemistry and Molecular Bioscience, University of Wollongong, Wollongong, NSW 2522, Australia

[2] Molecular Horizons, University of Wollongong, Wollongong, NSW 2522, Australia

[3] Illawarra Health and Medical Research Institute, Wollongong, NSW 2522, Australia

Keywords DNA lesion · UV · Thymine dimer · Dewar isomer · Solvation effects · DFT

Abstract

Density functional theory calculations have been carried out to investigate the formation mechanism of the thymine-thymine (6–4) dimer ((6–4)TT), which is one of the main DNA lesions induced by ultraviolet radiation and is closely related to skin cancers. The DNA backbone was found to have non-negligible effects on the triplet reaction pathway, particularly the reaction steps involving substantial base rotations. The mechanism for the isomerisation from (6–4)TT to its Dewar valence isomer (DewarTT) was also explored, confirming the necessity of absorbing a second photon. In addition, the solvation effects were examined and showed considerable influence on the potential energy surface.

Introduction

Excessive exposure to ultraviolet (UV) solar radiation can cause DNA damage in skin cells that may lead to skin cancers including melanoma [1]. The current research shows that UV radiation initiates the formation of two classes of DNA lesions: cyclobutane pyrimidine dimers (CPDs) and pyrimidine-pyrimidone (6–4) photoproducts ((6–4)PPs), and their Dewar valence isomers (DewarPPs) (Scheme 1) [2-5]. These cytotoxic, mutagenic and carcinogenic DNA photoproducts are considered to be the main causes of skin cancer [2-4, 6, 7]. While the mechanism of CPD formation has been intensively studied both experimentally [8-14] and theoretically [15-19], the reaction pathway for the formation of (6–4)PP [13, 20-26] or DewarPP [22, 27-31] remains elusive. The (6–4)PPs are currently believed to be initiated by a [2+2] cycloaddition of the C5=C6 double bond of a 5' base (*e.g.*, thymine) with the

C4 carbonyl group of the neighboring 3' base, forming an oxetane intermediate. The subsequent ring opening and proton (H3') transfer reactions then lead to the (6–4)PP photoproducts. Upon exposure to UV-A/B light (280–360 nm), the (6–4) lesions could rearrange to form DewarPPs [32] and could be converted back to (6–4)PPs at 240 nm [33] (Scheme 1).

Although DNA bases have strong UV absorption, DNA is intrinsically photo-stable and the efficiency of photolesion formation is less than 1% [21]. Most excited states undergo relaxation back to the ground state through various pathways such as internal conversion (IC) and intersystem crossing (ISC) [21, 34]. The ISC leads to the population of low-lying triplet excited states. Despite a low quantum yield of formation, the longer-lived triplet states are of paramount importance in the study of DNA photodamage [11, 18, 34, 35]. Recently, Yang *et al.* reported a density functional theory (DFT) study on the mechanism of thymine-thymine (6–4) dimer ((6–4)TT) formation on the lowest-lying triplet excited-state surface, as well as the interaction between the lowest-lying triplet and singlet states [24]. A stepwise pathway was predicted on the triplet potential energy surface (PES). However, neglect of the influence from the DNA backbone and the complementary strand may bring inaccuracies to the result. In this paper, we aim to investigate the effect of DNA backbone on the triplet mechanism of (6–4)TT dimer formation. The biggest discrepancy comes from the proton transfer reaction in the last step, which is subjected to a considerable energy barrier (15.8 kcal mol^{-1}) in our calculations, whereas it was previously predicted to be barrierless [24]. Our findings thus demonstrate the importance of backbone effect in the study of DNA photochemistry. In addition, we predicted the energy profile for the isomerization between (6–4)TT and its Dewar valence isomer (DewarTT), confirming that a second photon is needed to surmount the huge energy barrier.

Computational details

A model containing two thymines connected by a truncated sugar-phosphate backbone capped by hydrogen atoms (Fig. 1) was used to investigate the (6–4)TT lesion formation reaction. The thymines in the 5' or 3' end were represented as **T** and **T'**, respectively (Fig. 1). The initial structures for the reactant (normal thymines) and product (thymine dimer) were built by cutting the atoms needed in the model from crystal structures of DNA (6–4) photolyase with a (6–4)TT lesion after (PDB code: 3CVY [36]) and before repair (PDB code: 3CVU[36]), respectively. All the geometry optimizations were carried out at the (U)M06-2X/def2-SVP level of theory with no constraints. The obtained stationary points were characterized by frequency calculations. The M06-2X density functional has been shown to work well for noncovalent interactions [37], such as the DNA interbase interaction in our case, and the def2-SVP basis set is a robust choice for explorative structure optimizations considering the

computational cost [38]. The IEFPCM model [39] was adopted to consider solvation effects. Besides using the solvent with ε = 4.3 that simulates the aploar surroundings of the thymines, we also investigated the case with water (ε = 78.4) as the solvent, as our model involves the DNA backbone, which is exposed in an aqueous solution in physiological conditions. The crossing point (CP) was obtained with the minimum energy crossing point (MECP) method [40] as implemented in the sobMECP program [41], considering the interaction between the triplet diradical state and the singlet diradical state. The single-point energies and Mulliken spin densities were calculated at the optimised geometries at the M06-2X/def2-TZVPP level, and were used for comparison with Ref [24]. The zero-point vibrational energy (ZPE) corrections were not included in the PES calculations in order to compare energy with the crossing point (CP), which was obtained by the MECP method involving no ZPE corrections. All calculations were performed with the Gaussian 09 program suite [42].

Results and discussion

The triplet reaction pathway from normal thymines (**R1**) to (6–4)TT (**P1**), along with the optimized structures, is shown in Scheme 2 and Fig. 2. Firstly, O4' in **T'** approaches C5 and forms the diradical intermediate **I1**, in which the C5–O4' bond is formed ($d_{C5–O4'}$ = 1.469 Å) and the distance between C6 and C4' significantly shortens to 2.845 Å compared to 3.633 Å in **R1**. Meanwhile the C5–C6 bond shortens slightly (Δd = 0.012 Å), while the C4'–O4' elongates considerably by 0.139 Å. In the next step, the C6–C4' single bond is formed ($d_{C6–C4'}$ = 1.585 Å) via **TS2**, resulting in the oxetane intermediate **I2**. Subsequently, the C4–O4' bond breaks and the oxetane ring opens, accompanied by the proton transfer from N3' to O4'. The final product **P1** features a C6–C4' σ-bond (1.518 Å) and a buckled thymine ring (**T**, $d_{C5–C6}$ = 1.547 Å) with an extra hydroxyl group. These structures are generally analogous to those obtained with the simplified model [24], but the torsion angles between the two thymines may exhibit greater differences. We cannot make a further comparison as the detailed geometric parameters were not provided in Ref [24].

As displayed in Fig. 3, the energy profile of the above stepwise reaction shows significant difference from that reported in Ref [24]. The energy barrier for the first step (18.2 kcal mol^{-1}) is nearly 6 kcal mol^{-1} higher. Particularly, our calculation indicates an energy barrier of 15.8 kcal mol^{-1} for the proton transfer reaction (ΔE_{PT}, **I2** to **P1** via **TS3**), which was previously predicted as barrierless. This is probably due to the constraint originating from the backbone, as the proton transfer process involves dramatic rotation of both thymines. The existence of the backbone confines free rotation of the bases. To further verify this hypothesis, we removed the sugar-phosphate backbone from the optimized structures of **I2, TS3** and **P1**, and carried out further geometry optimizations at UB3LYP/6-31G(d,p).

The structures reported in Ref [24] were reproduced for **I2** and **P1**, but a different **TS3** with even lower energy was obtained (Fig. S1). The ΔE_{PT} in this case was calculated to be –2.8 kcal mol^{-1} and thus features a similar barrierless intramolecular proton transfer. Therefore, the geometric constraint caused by the backbone should be the main reason that leads to the discrepancy in ΔE_{PT} values.

Similar to the previous work [24], the transition from the diradical intermediate **I1** to the ring-closed species **I2** needs to overcome a prohibitively high energy barrier (35.7 kcal mol^{-1}) with great endothermicity (ΔE = 24.8 kcal mol^{-1}). Therefore, we also investigated the interaction between triplet and singlet diradical states close to **I1** to probe the possibility of ring closure via the singlet reaction channel. The MECP method was adopted to locate the spin crossover point (**CP**), which is only 1.0 kcal mol^{-1} higher in energy than **I1** and could be facilely reached. **CP** is close to **I1** in structure (Fig. S1a) with all atom positional root-mean-square deviation (RMSD) < 0.19 Å (Fig. S1b). A similar oxetane intermediate **SI2** (Fig. 4) is formed after the crossing point along the singlet pathway, and this process is highly exothermic (ΔE = –46.2 kcal mol^{-1}). The formation of the final (6–4)TT product (**SP1**) is subjected to an energy barrier of 17.9 kcal mol^{-1}, which involves significant geometric changes, such as ring opening of the oxetane moiety and the stretching of the C6–C5 bond (**STS3**, Fig. 4). Therefore, the singlet-triplet coupling via ISC circumvents the prohibitively high energy barrier in the triplet PES (**I1** to **I2**) and makes the triplet mechanism possible.

As (6–4)TT could be converted to its valence isomer DewarTT (**D1**) at 313 nm [33], we continued our PES study and mapped out possible pathways to further understand this isomerization process. As shown in Scheme 3, we considered a transition state (**TS4**) with a buckled thymine (**T'**), in which N3' and C6' are approaching each other. The energy profile and the corresponding structures for both singlet and triplet routes are provided in Figs. 3 and 5, respectively. While both having rather high reaction barriers, the triplet channel displays a lower value (60.9 kcal mol^{-1}) compared to that of the singlet pathway (91.8 kcal mol^{-1}). As the above result supports **SP1** to be the final product of (6–4)TT formation reaction, we suggest that the DewarTT could be formed via the singlet pathway by absorbing a second photon with λ_{max} of 311 nm (~ 92 kcal mol^{-1}), which is consistent with the experiment [33].

It is worth mentioning that the system needs to be excited from the ground-state singlet species to the triplet state **R1** as the initial reactant via ISC. When looking into the geometry of **R1**, we found the 5' thymine (**T**) manifests a slightly buckled structure (Fig. 2) with an elongation of the C6–C5 bond (1.498 Å) and C4–O4 bond (1.224 Å), while the other thymine (**T'**) remains a normal planar structure. As a result, the spin densities of **R1** mainly (98% of total) reside on **T**, with substantial localization on

C5 (0.80), C6 (0.80) and O4 (0.21). As shown in Fig. 6, the spin densities gradually transfer from **T** to **T'**, which is consistent with that reported in Ref [24]. Summing up the total spin densities separately (Table 1), we find they are almost exclusively localized on the thymines (> 97%), with negligible distribution on the backbone (< 3%). Thus the backbone should influence the lesion formation reaction mainly via geometric constraint effect with insignificant electronic contribution.

In the previous study using a model containing no backbone [24], bulk solvation with $\varepsilon = 4.3$ was used to mimic the aploar environment and only marginal influence on the energy barrier was found due to the solvation effects. Since the sugar-phosphate backbone in our model is exposed in an aqueous solution in physiological conditions, we also computed the PES with water ($\varepsilon = 78.4$) as the solvent. As shown in Table 2, in the case of $\varepsilon = 4.3$, solvation effects cause a big increase in the relative energy of **TS3** (5.3 kcal mol^{-1}), **P1** (2.2 kcal mol^{-1}) and **STS3** (3.0 kcal mol^{-1}), while the energy change is less than 1.5 kcal mol^{-1} in all the other species. The result using water as the solvent shows a similar trend in energy change, but to a greater extent. Therefore, our computations suggest a considerable influence of the solvation effects on the PES of such backbone-base system.

Conclusions

DFT calculations using a model with two thymines connected by a DNA backbone were carried out to investigate the triplet reaction pathway for DNA (6–4)TT lesion formation. While the previous work predicted a PES based on a simplified model system only containing two thymines, our results demonstrate some different features. Particularly our computation suggests an energy barrier of 15.8 kcal mol^{-1} for the proton transfer step on the triplet PES, whereas it was predicted as barrierless previously. This indicates the constraint caused by the backbone should have nonnegligible influence on the reaction pathway, especially the reaction steps involving considerable rotation of bases. Together with the profile of spin density distribution, which is mainly localized on the thymines, we believe the backbone should influence the reaction primarily through geometric effect instead of electronic effect. On the other hand, using a more sophisticated method (MECP) for the search of spin crossover point, we also find that the singlet-triplet interaction via ISC is crucial to the formation of the (6–4)TT photoproduct. The solvation effects were found to have considerable influence on the energy profile of the reaction. Finally, a possible reaction pathway for the rearrangement from (6–4)TT to DewarTT was explored, in which the absorption of a second photon was needed. Further study on the influence from the complementary strand (*e.g.*, base pairing effect), which requires a larger model and thus is more challenging, is under way.

Acknowledgements

H.Y. is the recipient of an Australian Research Council Future Fellowship (Project number FT110100034) and X.W. is the recipient of the University of Wollongong Vice Chancellor's Postdoctoral Research Fellowship. We wish to acknowledge that this research was undertaken with the assistance of resources provided at the NCI National Facility Systems at the Australian National University through the National Computational Merit Allocation Scheme supported by the Australian Government (project id uq5 and v15).

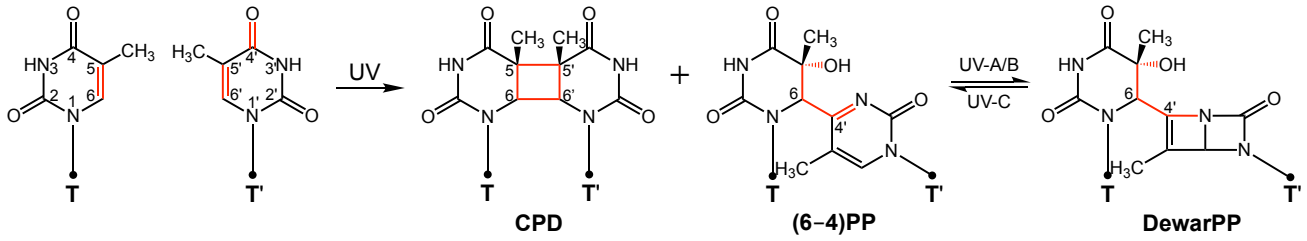

Scheme 1 A molecular scheme of DNA photodamage induced by UV radiation. The reaction center is highlighted in red and the sugar-phosphate backbone is not displayed for clarity. The thymine-thymine (6–4) dimer is used here as an example of DNA lesions.

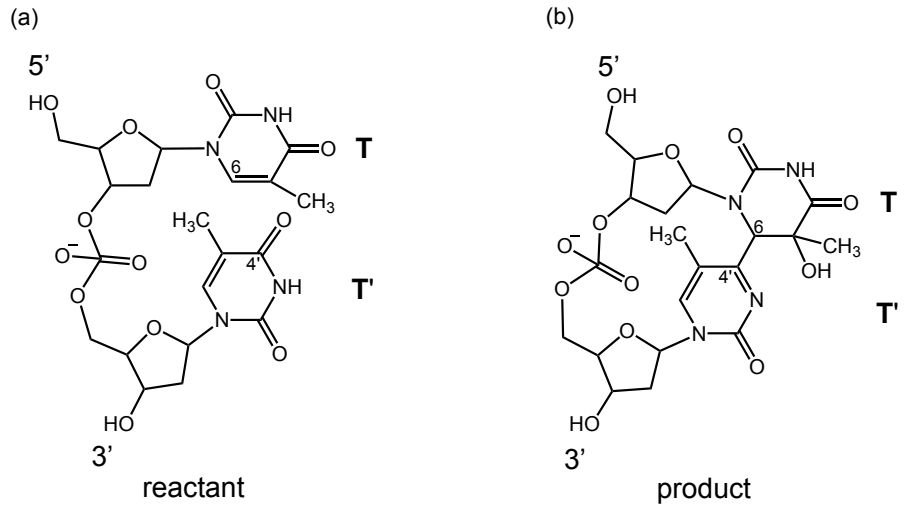

Fig. 1 The models for the (a) reactant and (b) product used in this paper, with either two normal thymines or a thymine dimer. The 5' and 3' thymines are denoted as **T** and **T'**, respectively.

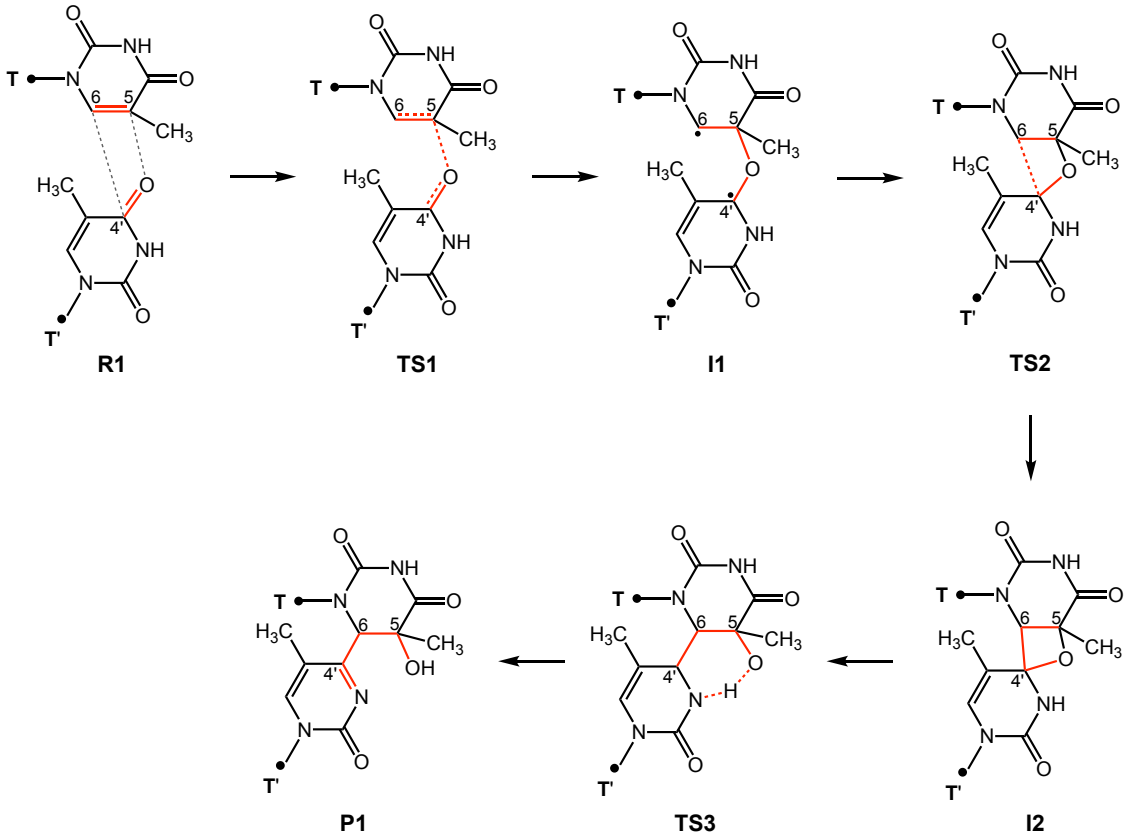

Scheme 2 The reaction pathway for the triplet mechanism of thymine-thymine (6–4) dimerization. The sugar-phosphate backbone is not displayed for clarity.

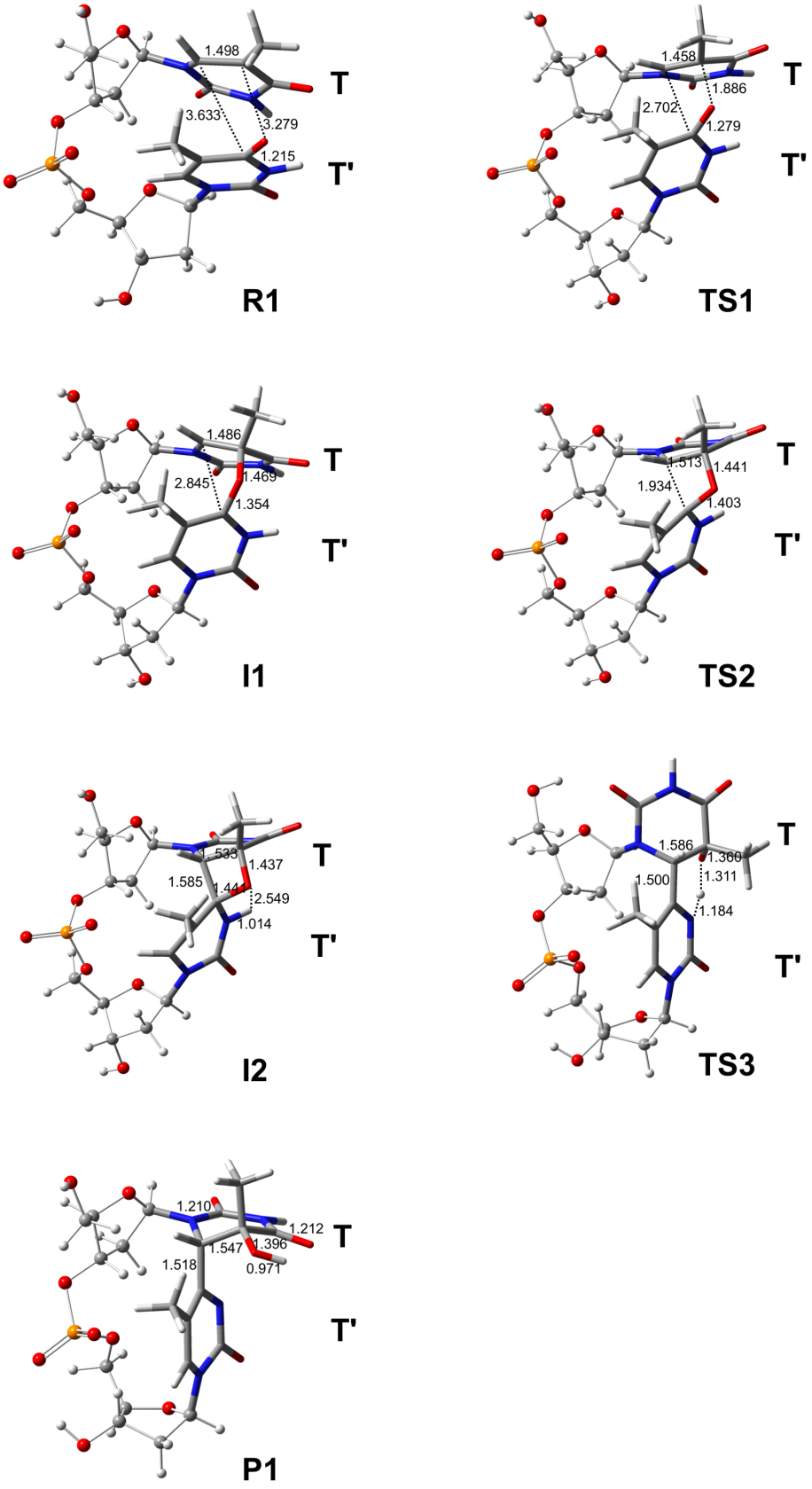

Fig. 2 Optimized structures along the triplet pathway for (6–4)TT formation with selected bond lengths (Å). The thymines and sugar-phosphate backbone are displayed as tube and ball-and-stick representations respectively for clearer view.

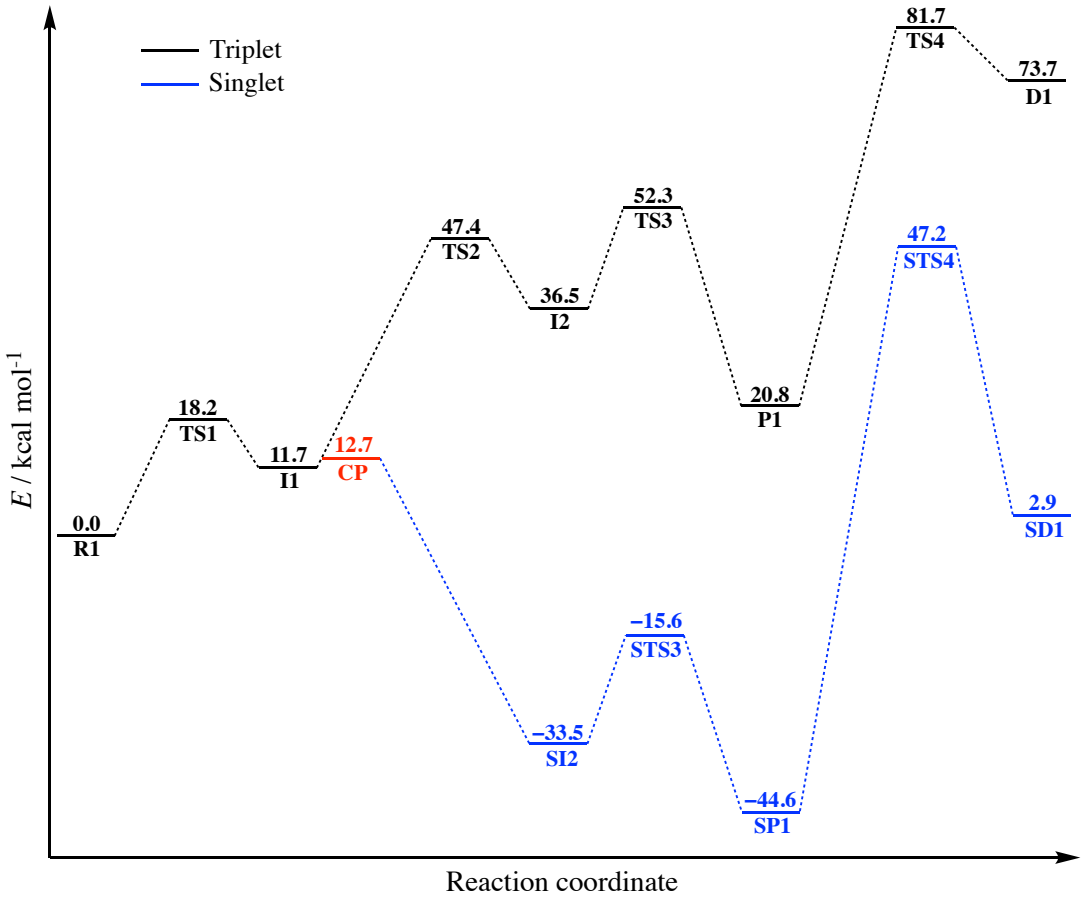

Fig. 3 Potential energy profiles calculated at the (U)M06-2X/def2-TZVPP level for (6–4)TT formation along both triplet and singlet reaction pathways, where the intersystem crossing occurs at the crossing point (**CP**).

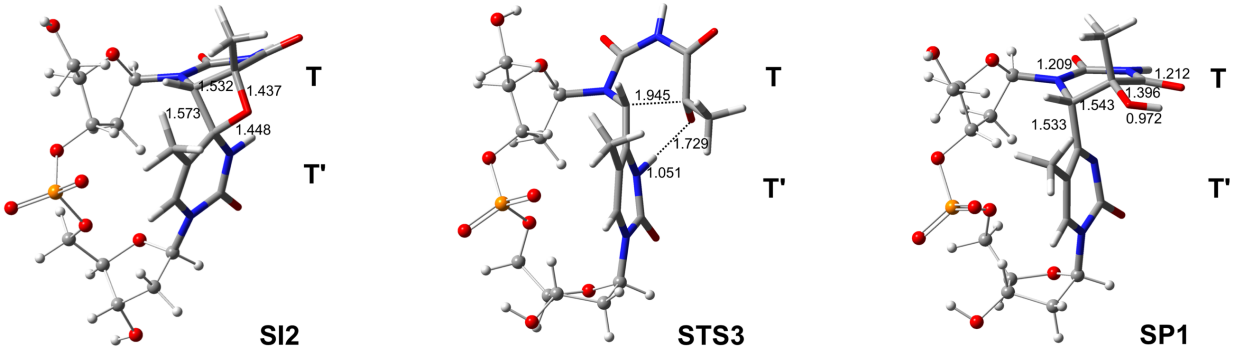

Fig. 4 Optimized structures for the proton transfer reaction along the singlet pathway with selected bond lengths (Å).

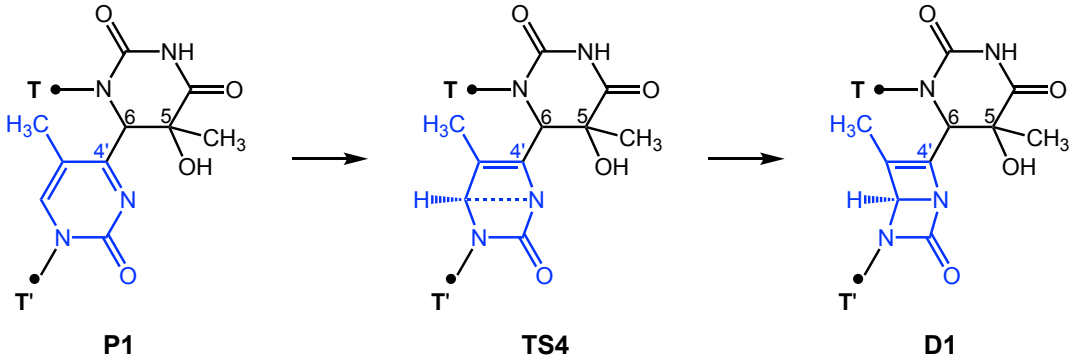

Scheme 3 The reaction pathway for the isomerisation between (6–4)TT and its Dewar valence isomer (DewarTT). The sugar-phosphate backbone is not displayed for clarity.

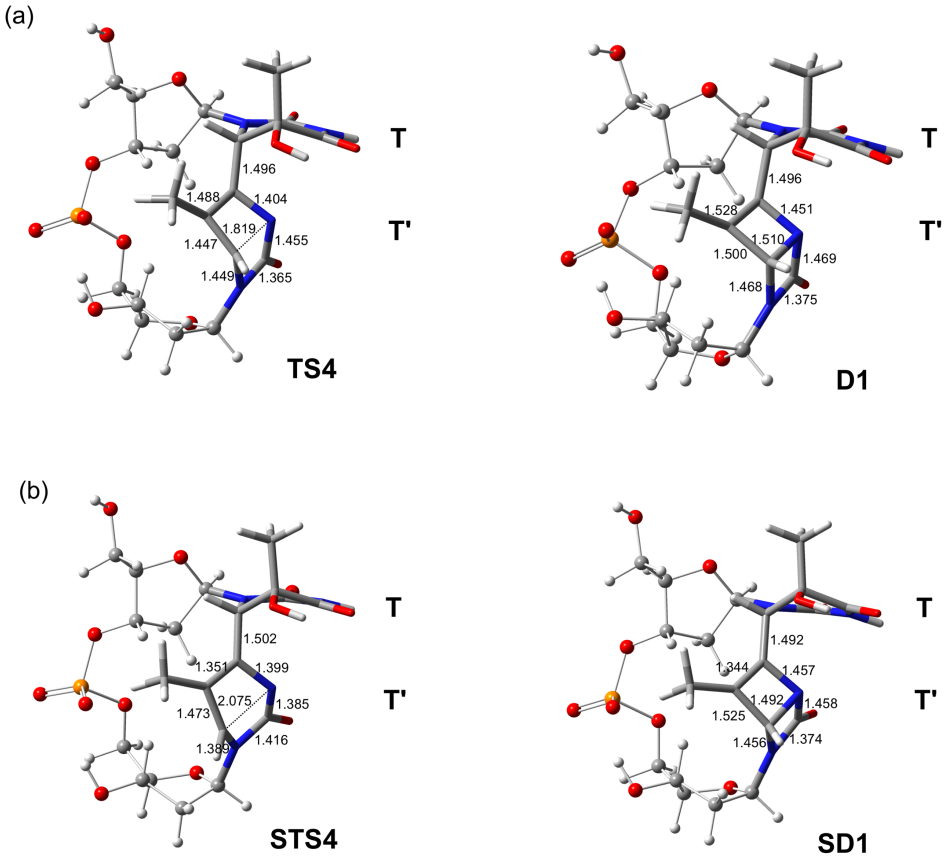

Fig. 5 Optimized structures for the formation of DewarTT along either (a) triplet or (b) singlet pathway with selected bond lengths (Å).

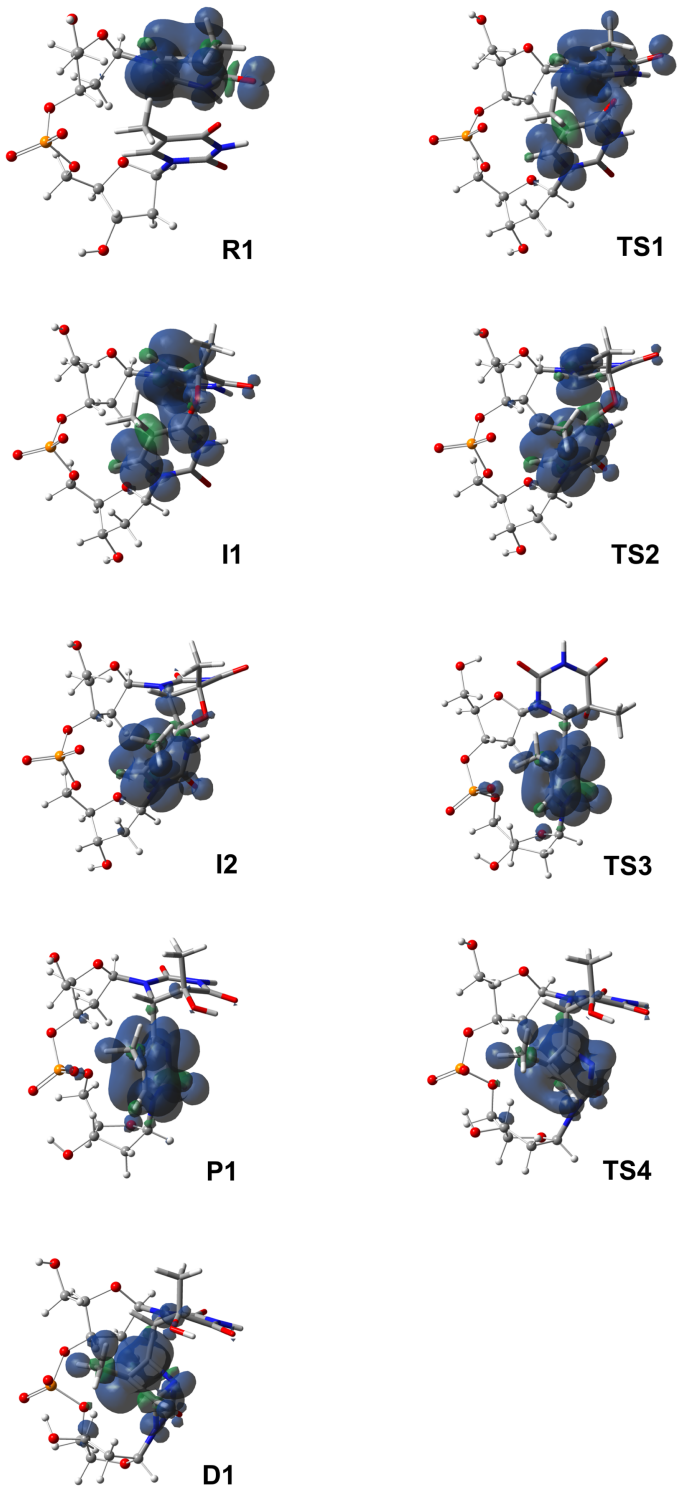

Fig. 6 Spin density distributions calculated at the UM06-2X/Def2-TZVPP level for the species along the triplet reaction pathway drawn at isovalue of 0.002 e^{-}/Bohr^3.

Table 1. Mulliken spin densities (e^-) of the thymines and the backbone for species along the triplet thymine-thymine cycloaddition pathway calculated at the UM06-2X/Def2-TZVPP level.

	Thymines	Backbone
R1	1.967	0.033
TS1	1.979	0.022
I1	1.970	0.030
CP	1.958	0.042
TS2	1.991	0.009
I2	1.996	0.004
TS3	1.984	0.016
P1	1.977	0.023
TS4	1.966	0.034
D1	1.949	0.051

Table 2. Relative energies (without ZPE corrections, in kcal mol^{-1}) obtained with different solvents calculated at the (U)M06-2X/Def2-TZVPP/IEFPCM level compared with the gas phase values.

	Gas phase	$\varepsilon = 4.3$	Water ($\varepsilon = 78.4$)
R1	0.0	0.0	0.0
TS1	18.2	17.0	16.1
I1	11.7	10.5	9.8
CP	12.7	11.6	11.0
TS2	47.4	46.2	45.5
I2	36.5	35.4	34.7
TS3	52.3	57.6	58.7
P1	20.8	23.0	23.6
TS4	81.7	81.3	80.6
D1	73.7	73.4	72.7
SI2	−33.5	−34.7	−35.5
STS3	−15.6	−12.6	−11.8
SP1	−44.6	−43.5	−43.4
STS4	47.2	45.8	44.6
SD1	2.9	1.7	0.6

References

1 Friedberg EC, Walker GC, Siede W, Wood RD, Schultz RA, Ellenberger T (2006) DNA repair and mutagenesis. ASM Press: Washington, DC.

2 Taylor JS (1994) Unraveling the molecular pathway from sunlight to skin-cancer. Acc Chem Res 27(3):76-82.

3 Ravanat JL, Douki T, Cadet J (2001) Direct and indirect effects of UV radiation on DNA and its components. J Photoch Photobio B 63(1-3):88-102.

4 Douki T, Cadet J (2001) Individual determination of the yield of the main UV-induced dimeric pyrimidine photoproducts in DNA suggests a high mutagenicity of CC photolesions. Biochemistry 40(8):2495-2501.

5 Lukin M, de los Santos C (2006) NMR structures of damaged DNA. Chem Rev 106(2):607-686.

6 Lima-Bessa KM, Menck CFM (2005) Skin cancer: Lights on genome lesions. Curr Biol 15(2):R58-R61.

7 Sinha RP, Hader DP (2002) UV-induced DNA damage and repair: a review. Photoch Photobio Sci 1(4):225-236.

8 Marguet S, Markovitsi D (2005) Time-resolved study of thymine dimer formation. J Am Chem Soc 127(16):5780-5781.

9 Mouret S, Baudouin C, Charveron M, Favier A, Cadet J, Douki T (2006) Cyclobutane pyrimidine dimers are predominant DNA lesions in whole human skin exposed to UVA radiation. P Natl Acad Sci USA 103(37):13765-13770.

10 Schreier WJ, Schrader TE, Koller FO, Gilch P, Crespo-Hernandez CE, Swaminathan VN, Carell T, Zinth W, Kohler B (2007) Thymine dimerization in DNA is an ultrafast photoreaction. Science 315(5812):625-629.

11 Kwok WM, Ma C, Phillips DL (2008) A doorway state leads to photostability or triplet photodamage in thymine DNA. J Am Chem Soc 130(15):5131-5139.

12 Cuquerella MC, Lhiaubet-Vallet V, Bosca F, Miranda MA (2011) Photosensitised pyrimidine dimerisation in DNA. Chem Sci 2(7):1219-1232.

13 Banyasz A, Douki T, Improta R, Gustavsson T, Onidas D, Vaya I, Perron M, Markovitsi D (2012) Electronic excited states responsible for dimer formation upon UV absorption directly by thymine strands: joint experimental and theoretical study. J Am Chem Soc 134(36):14834-14845.

14 Lee JH, Choi YJ, Choi BS (2000) Solution structure of the DNA decamer duplex containing a 3 '-T.T base pair of the cis-syn cyclobutane pyrimidine dimer: implication for the mutagenic property of the cis-syn dimer. Nucleic Acids Res 28(8):1794-1801.

15 Zhang RB, Eriksson LA (2006) A triplet mechanism for the formation of cyclobutane pyrimidine dimers in UV-irradiated DNA. J Phys Chem B 110(14):7556-7562.

16 Serrano-Perez JJ, Gonzalez-Ramirez I, Coto PB, Merchan M, Serrano-Andres L (2008) Theoretical insight into the intrinsic ultrafast formation of cyclobutane pyrimidine dimers in UV-irradiated DNA: thymine versus cytosine. J Phys Chem B 112(45):14096-14098.

17 Roca-Sanjuan D, Olaso-Gonzalez G, Gonzalez-Ramirez I, Serrano-Andres L, Merchan M (2008) Molecular basis of DNA photodimerization: Intrinsic production of cyclobutane cytosine dimers. J Am Chem Soc 130(32):10768-10779.

18 Climent T, Gonzalez-Ramirez I, Gonzalez-Luque R, Merchan M, Serrano-Andres L (2010) Cyclobutane pyrimidine photodimerization of DNA/RNA nucleobases in the triplet state. J Phys Chem Lett 1(14):2072-2076.

19 Barbatti M (2014) Computational reference data for the photochemistry of cyclobutane pyrimidine dimers. ChemPhysChem 15(15):3342-3354.

20 Blancafort L, Migani A (2007) Modeling thymine photodimerizations in DNA: mechanism and correlation diagrams. J Am Chem Soc 129(47):14540-14541.

21 Middleton CT, de La Harpe K, Su C, Law YK, Crespo-Hernandez CE, Kohler B (2009) DNA excited-state dynamics: from single bases to the double helix. Annu Rev Phys Chem 60:217-239.

22 Ai YJ, Liao RZ, Chen SF, Luo Y, Fang WH (2010) Theoretical studies on photoisomerizations of (6-4) and dewar photolesions in DNA. J Phys Chem B 114(44):14096-14102.

23 Yang ZB, Eriksson LA, Zhang RB (2011) A theoretical rationale for why azetidine has a faster rate of formation than oxetane in TC(6-4) photoproducts. J Phys Chem B 115(31):9681-9686.

24 Yang ZB, Zhang RB, Eriksson LA (2011) A triplet mechanism for the formation of thymine-thymine (6-4) dimers in UV-irradiated DNA. Phys Chem Chem Phys 13(19):8961-8966.

25 Giussani A, Serrano-Andres L, Merchan M, Roca-Sanjuan D, Garavelli M (2013) Photoinduced formation mechanism of the thymine-thymine (6-4) adduct. J Phys Chem B 117(7):1999-2004.

26 Giussani A, Conti I, Nenov A, Garavelli M (2018) Photoinduced formation mechanism of the thymine-thymine (6-4) adduct in DNA; a QM(CASPT2//CASSCF):MM(AMBER) study. Faraday Discuss 207:375-387.

27 Ai YJ, Liao RZ, Chen SL, Hua WJ, Fang WH, Luo Y (2011) Repair of DNA Dewar photoproduct to (6-4) photoproduct in (6-4) photolyase. J Phys Chem B 115(37):10976-10982.

28 Haiser K, Fingerhut BP, Heil K, Glas A, Herzog TT, Pilles BM, Schreier WJ, Zinth W, de Vivie-Riedle R, Carell T (2012) Mechanism of UV-induced formation of dewar lesions in DNA. Angew Chem Int Ed 51(2):408-411.

29 Fingerhut BP, Herzog TT, Ryseck G, Haiser K, Graupner FF, Heil K, Gilch P, Schreier WJ, Carell T, de Vivie-Riedle R, Zinth W (2012) Dynamics of ultraviolet-induced DNA lesions: Dewar formation guided by pre-tension induced by the backbone. New J Phys 14(6):065006.

30 Bucher DB, Pilles BM, Carell T, Zinth W (2015) Dewar lesion formation in single- and double-stranded DNA is quenched by neighboring bases. J Phys Chem B 119(28):8685-8692.

31 Douki T, Rebelo-Moreira S, Hamon N, Bayle PA (2015) DNA photochemistry: geometrically unconstrained pyrimidine (6-4) pyrimidone photoproducts do photoisomerize. Org Lett 17(2):246-249.

32 Taylor JS, Garrett DS, Cohrs MP (1988) Solution-state structure of the dewar pyrimidinone photoproduct of thymidylyl-(3'-]5')-thymidine. Biochemistry 27(19):7206-7215.

33 Johns HE, Pearson ML, LeBlanc JC, Helleiner CW (1964) The ultraviolet photochemistry of thymidylyl-(3'→5') thymidine. J Mol Biol 9(2):503-523.

34 Merchan M, Serrano-Andres L, Robb MA, Blancafort L (2005) Triplet-state formation along the ultrafast decay of excited singlet cytosine. J Am Chem Soc 127(6):1820-1825.

35 Hare PM, Middleton CT, Mertel KI, Herbert JM, Kohler B (2008) Time-resolved infrared spectroscopy of the lowest triplet state of thymine and thymidine. Chem Phys 347(1-3):383-392.

36 Maul MJ, Barends TRM, Glas AF, Cryle MJ, Domratcheva T, Schneider S, Schlichting I, Carell T (2008) Crystal structure and mechanism of a DNA (6-4) photolyase. Angew Chem Int Ed 47(52):10076-10080.

37 Zhao Y, Truhlar DG (2007) The M06 suite of density functionals for main group thermochemistry, thermochemical kinetics, noncovalent interactions, excited states, and transition elements: two new functionals and systematic testing of four M06-class functionals and 12 other functionals. Theor Chem Acc 120(1-3):215-241.

38 Weigend F, Ahlrichs R (2005) Balanced basis sets of split valence, triple zeta valence and quadruple zeta valence quality for H to Rn: Design and assessment of accuracy. Phys Chem Chem Phys 7(18):3297-3305.

39 Mennucci B, Tomasi J (1997) Continuum solvation models: A new approach to the problem of solute's charge distribution and cavity boundaries. J Chem Phys 106(12):5151-5158.

40 Harvey JN, Aschi M, Schwarz H, Koch W (1998) - The singlet and triplet states of phenyl cation. A hybrid approach for locating minimum energy crossing points between non-interacting potential energy surfaces. Theor Chem Acc 99(2):95-99.

41 Lu T, sobMECP program, http://sobereva.com/286 (accessed on March 2017).

42 Frisch MJ, Trucks GW, Schlegel HB, Scuseria GE, Robb MA, Cheeseman JR, Scalmani G, Barone V, Mennucci B, Petersson GA, Nakatsuji H, Caricato M, Li X, Hratchian HP, Izmaylov AF, Bloino J, Zheng G, Sonnenberg JL, Hada M, Ehara M, Toyota K, Fukuda R, Hasegawa J, Ishida M, Nakajima T, Honda Y, Kitao O, Nakai H, Vreven T, Montgomery JA, Jr., Peralta JE, Ogliaro F, Bearpark M, Heyd JJ, Brothers E, Kudin KN, Staroverov VN, Keith T, Kobayashi R, Normand J, Raghavachari K, Rendell A, Burant JC, Iyengar SS, Tomasi J, Cossi M, Rega N, Millam JM, Klene M, Knox JE, Cross JB, Bakken V, Adamo C, Jaramillo J, Gomperts R, Stratmann RE, Yazyev O, Austin AJ, Cammi R, Pomelli C, Ochterski JW, Martin RL, Morokuma K, Zakrzewski VG, Voth GA, Salvador P, Dannenberg JJ, Dapprich S, Daniels AD, Farkas O, Foresman JB, Ortiz JV, Cioslowski J, Fox DJ (2013) Gaussian 09, Revision D.01, Gaussian, Inc., Wallingford CT.

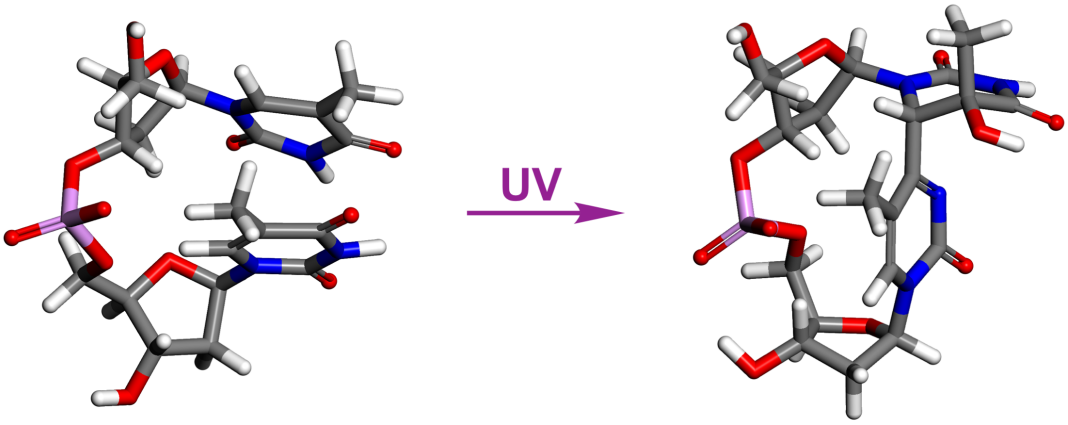

Graphical Abstract

DFT calculations on the influence of DNA backbone on the mechanism of UV-induced thymine-thymine (6–4) dimer formation